Heliyon 6 (2020) e03293

Contents lists available at ScienceDirect

Heliyon

journal homepage: www.cell.com/heliyon

Research article

Photocatalytic degradation of swine wastewater on aqueous TiO_2 suspensions: optimization and modeling via Box-Behnken design

Bruno B. Garcia, G. Lourinho *, P. Romano, P.S.D. Brito

VALORIZA - Research Center for Endogenous Resource Valorization, Campus Politécnico, 10, 7300-555, Portalegre, Portugal

ARTICLE INFO

Keywords:
Heterogeneous catalysis
Photocatalysis
Waste treatment
Wastewater management
Water treatment
Swine wastewater
Titanium dioxide
Optimization
Kinetics

ABSTRACT

Heterogeneous photocatalysis is a promising technology to treat many industrial wastewaters. To date, this potential has not been proven with wastewaters from agricultural origins, such as swine wastewater. In this work, the photocatalytic degradation of swine wastewater was studied by applying a response surface methodology based on the Box-Behnken design. The interactive effects of the variation of factors such as photocatalyst dosage (X_1), wastewater concentration (X_2), and irradiation time (X_3) were analyzed to identify the optimal operating conditions for COD reduction. A second-order polynomial accurately represented organics degradation with a high adjusted R-squared (0.9666). The main effects of factor X_2 and the quadratic effects of factors X_2 and X_3 were the most significant for COD reduction. The optimal conditions for COD degradation were 1.16 g L^{-1} for photocatalyst dosage, 1.68% for wastewater concentration, and irradiation time of 9.2 h. These results have been validated in a confirmation experiment and COD removal reached 91.7% (98.1 % predicted). Based on the Langmuir—Hinshelwood model, the reaction rate constant was 3.9×10^{-3} min^{-1}. Besides, FTIR analysis indicated that Aeroxide® TiO_2 reusability may be possible, especially for low wastewater concentrations. Heterogeneous photocatalysis can be applied as a technology for the integrated treatment of industrial wastewaters resulting from swine production.

1. Introduction

The meat production industry has expanded rapidly in recent decades with severe implications for public health and the environment. Animal wastes, especially swine wastewater, release gaseous emissions (NH_3, N_2O, and CH_4) that originate from animal buildings and manure storage [1, 2]. Besides, livestock production is associated with a high-water consumption by accounting for roughly 23 percent of global water use in agriculture [3]; as a consequence, high amounts of wastewater are generated in intensive swine farms, thus needing an adequate treatment to meet environmental regulations. In particular, swine wastewater (SWW) usually contains high concentrations of organic matter, suspended solids, nitrogen and phosphorus compounds, which can cause water pollution and overfertilization of soils. Also, these effluents are a source of virus and protozoan pathogens, which can cause disease in both animals and humans [4].

In this context, multiple technologies have been applied to SWW remediation in large farms. Biological methods, either aerobic or anaerobic, are by far the most popular as they are usually economical, practical and offer the possibility of energy recovery. However, these techniques are also time-consuming (high retention times) and very sensitive to process conditions (organic loading rates, ammonia accumulation), which can easily lead to treatment failure. As an alternative, advanced oxidation processes (AOPs) have been gaining interest as new and promising treatment technologies for many industrial wastewaters [5, 6, 7]. Among AOPs, heterogeneous photocatalysis using solid semiconductors as photocatalysts have been widely studied. The underlying mechanism of the photooxidation process is well known and involves the stimulation of the photocatalyst surface by a UV light source (λ = 320–400 nm). This stimulation causes a valence band electron of the semiconductor to be excited to the conduction band surface, and photo-induced holes are generated as a consequence. After a series of photochemical reactions, reactive oxygen species (ROS) such as hydroxyl and superoxide radicals can be produced. The highly oxidizing and non-selective hydroxyl radicals are active for the degradation of pollutants and may lead to the complete mineralization of organic compounds or the formation of biodegradable intermediate compounds [8, 9].

Titanium dioxide (TiO_2) is considered the most effective semiconductor material for the oxidation of organic pollutant molecules due to excellent features such as high photocatalytic efficiency, physical and

* Corresponding author.
E-mail address: goncalo.lourinho@ipportalegre.pt (G. Lourinho).

https://doi.org/10.1016/j.heliyon.2020.e03293
Received 12 November 2019; Received in revised form 13 January 2020; Accepted 21 January 2020

chemical stability, low cost and low toxicity [10]. Good photocatalytic activities were reported using TiO_2 powders, but recent trends have called for TiO_2 immobilization on various substrates. For example, Sirirerkratana *et al.* [11] tested the photocatalytic activities of TiO_2 thin films coated on different substrate materials using dye-contaminated wastewater under UV irradiations. Their results showed that the better substrate (transparent glass) and light source (UVC) yielded the highest color removal efficiency (87.86 ± 0.23%) at pH 11. Maleisic-Eleftheriadou *et al.* [12] used recycled polyethylene terephthalate (PET) as a supporting polymer for commercial TiO_2 immobilization. They investigated the photocatalytic activity of these bio-based TiO_2 composite films under simulated solar irradiation for the degradation of several antibiotics with encouraging results. Indeed, most of the studied antibiotics were almost completely degraded within 2 h of irradiation. Based on this, TiO_2 is still a widely researched photocatalyst especially at a pre-industrial scale where the well-known features of commercial photocatalysts have allowed more *in situ* experimental studies [13].

Although TiO_2 is the most commonly reported photocatalyst in the literature, some efforts have been devoted to constructing novel materials with improved photocatalytic activities. In particular, research has focused on overcoming TiO_2 limitations by using several strategies to reduce the fast recombination rate of electron-hole pairs and extend light absorption to the visible part of the spectrum [14]. Among these strategies, the fabrication of heterojunction visible-light photocatalysts has been a popular approach. The reason is that this heterostructure is advantageous to the spatial separation of photo-induced electron-hole pairs, thus enhancing photocatalytic performance [14]. From the literature, some recent studies targeting the degradation of organic contaminants by using different types of heterogeneous junctions are worth mentioning. For example, Li *et al.* [15] and Wang *et al.* [16] constructed BP/BiOBr and $SnFe_2O_4/ZnFe_2O_4$ heterojunctions for the effective toxicity elimination of tetracycline and its intermediates with outstanding performance. The enhanced photocatalyst properties could be attributed to the formation of S-scheme heterojunction which boosted the charge separation ability of the composite photocatalysts. On the basis of Z-scheme heterojunctions, other researchers have developed promising photocatalysts based on copper indium disulfide ($CuInS_2$) [17] and bismuth oxybromide (BiOBr) [18] composites with enhanced visible-light utilization and good photocatalytic features towards the treatment of real pharmaceutical wastewaters. Nevertheless, despite many advances, these photocatalysts are still far away from practical and commercial applications.

Based on the existing literature, photocatalytic technologies have been frequently performed to degrade organic dyes and pharmaceuticals present in wastewater streams [9, 16, 17, 18, 19, 20, 21]; however, despite some studies, the treatment of dirty wastewaters from agro-industrial origin has been underexplored [6, 22, 23]. Therefore, the novelty of our work lies in the use of heterogeneous photocatalysis to treat organic effluents from swine production. Indeed, to the best of our knowledge, no other research has been conducted that uses SWW. In particular, this study aims to demonstrate that photocatalysis can be integrated within the conventional treatment of wastewaters from agro-industrial origin by using a simple and commercially available photocatalyst such as TiO_2. In this context, it should be highlighted that the results obtained with this work can provide a basis for research intensification using SWW considering the most recent developments on the topic of photocatalysis. For example, commercial TiO_2 studies can be used to compare the photocatalytic efficiency of novel photocatalytic materials such as the heterojunction photocatalysts briefly discussed above. Considering these ideas, in this work, the degradation of organic pollutants present in SWW was studied under batch mode using SWW-TiO_2 mixtures in aqueous suspension. Response Surface Methodology (RSM) based on Box-Behnken design (BBD) was used to model the photocatalytic process and assess the influence of three operational parameters on COD reduction (Photocatalyst dosage, Wastewater concentration, and Irradiation time). The optimal operating conditions were applied in a confirmation experiment in order to validate the model and demonstrate the possible real application of photocatalytic technology to degrade SWW.

2. Materials and methods

2.1. Source of swine wastewater

The SWW used in this study was sampled from a large intensive swine production farm in Alentejo, Portugal. The farm raises 50,000 pigs per year and operates in a closed cycle, comprising nursing and fattening in a single production unit. The SWW samples (fattening phase) were collected from drainpipes that carried wastewater to the exterior before any treatment was applied and separated into supernatant and bottom sediment through gravity sedimentation. The obtained supernatant containing few suspended solids was homogenized and stored at 4.0 °C until used in the photocatalytic experiments. The main composition of SWW was as follows: pH, 7.85 ± 0.05; conductivity, 25.4 ± 2.88 mS cm^{-1}; TDS, 13.36 ± 0.72 mg L^{-1}; TS, 0.9 ± 0.1%; VS, 67.8 ± 2.3% TS; COD, 13109 ± 600 mg L^{-1}.

2.2. Chemicals and reagents

The powdered photocatalyst used in the experiments was commercial Aeroxide® TiO_2 P25 from Evonik Industries (70 % anatase: 30 % rutile). Due to its complex crystalline microstructure (average particle size of 21 nm) and high surface area of about 50 $m^2\ g^{-1}$ this semiconductor catalyst achieves a high photoactivity [8]. More characterization data of the material can be found elsewhere in the literature [24]. All SWW dilutions were prepared by using Milli-Q water.

2.3. Experimental design and photocatalytic experiments

The effect of three independent factors, i.e., Photocatalyst dosage (X_1), Wastewater concentration (X_2), and Irradiation time (X_3), on photocatalysis efficiency was investigated using a three-level BBD. Each selected factor was studied at three levels, low (-1), medium (0), and high (+1), for a total of 15 experiments (Table 1). R open-source software with R Commander (Rcmdr) package [25] was used for BBD design and statistical analysis of the experimental data as demonstrated by [26]. Functional relationships between response (Y) and the set of factors (X_1, X_2, and X_3) were inferred by fitting a second-order polynomial quadratic model of Eq. (1) based on experimental data. Analysis of variance (ANOVA) was used to evaluate the significance of results, and $p < 0.05$ was considered statistically significant.

Experiments were conducted in batch mode using 200 mL of SWW at various concentrations (3.125 %, 6.250 %, and 9.375 %). After preparation, samples were transferred to 500 mL beakers, and adequate amounts of TiO_2 were added depending on the experimental run (0.5 g L^{-1}, 1.0 g L^{-1}, 1.5 g L^{-1}). Before irradiation, each sample was stirred for 40 min, in the dark, to allow TiO_2 to disperse in the solution. The photocatalytic reaction was started by placing the samples under irradiation using a 125 W mercury vapor lamp (OSRAM HQL 125) as a radiation source. The mercury vapor lamp has enhanced emission in the low wavelength area covering UV (367 nm) and visible light (406, 438, 548

Table 1. Coded and actual values used for the photocatalysis optimization via the Box-Behnken design.

Variables	Coded and actual values		
	-1	0	1
X_1: Photocatalyst dosage (g L^{-1})	0.5	1	1.5
X_2: Wastewater concentration (%)	3.125	6.250	9.375
X_3: Irradiation Time	6	9	12

and 580 nm) intense lines [27] (Figure 1). UV radiation was collimated by using a light fixture (SBP Jolly 2/S 400 94) to assure the same radiation intensity was received by the samples (Figure 2). The distance from the lamp to the center of the beakers was 50 cm. Irradiation measurements were carried out at these conditions (10–15 W m^{-2}) using a radiometer (Acadus 85-PLS) with a measuring peak at 330 nm (75%), and a response range between 290 and 370 nm. The lamp was turned on for at least 45 min before experiments to ensure constant radiation output. After the desired experiment time (0, 6, 9, and 12 h), samples were centrifuged for 10 min at 10000 rpm, in the dark, and immediately analyzed for COD. Photodegradation experiments also had a comparative "blank experiment'' with no TiO_2 added so that photolytic degradation could be assessed.

2.4. TiO_2 reusability

Structural changes in Aeroxide® TiO_2 photocatalyst were examined using FTIR spectroscopy. After each run, the photocatalyst was separated from the SWW solution through centrifugation, washed thoroughly with deionized water and dried at 60 °C. FTIR spectra were obtained as a mean of 64 scans collected at a resolution of 32 cm^{-1} by using an ATR-FTIR spectrometer (Thermo Scientific Nicolet iS10) in the wavenumber range from 4000–400 cm^{-1}. Powdered photocatalyst samples were placed on the ATR crystal and compressed by using a flat axial screw for analysis.

2.5. Analytical methods

TS were determined gravimetrically after drying the samples for at least 24 h at 105 °C. VS were analyzed by loss on ignition at 550 °C for 2 h. The pH, conductivity, and TDS were measured by using a pH/conductivity/TDS meter (Hanna Instruments HI 9180). Total COD measurements were performed according to the closed reflux colorimetric method (5220 D) [28]. Appropriate amounts of SWW sample, digestion solution containing potassium dichromate and sulfuric acid reagent were introduced into digestion vials and kept at 150 °C for 2 h in a COD digestion unit (Aqualytic AL32). After cooling to room temperature, absorbance was measured for all samples using a UV-vis spectrophotometer at 600 nm (Turner, Model 690). Potassium hydrogen phthalate (Sigma-Aldrich) standard solutions were used to prepare a COD calibration curve in the range of 0 and 1000 mg L^{-1}. The efficiency of COD degradation was calculated via Eq. (1), where COD_0 and COD are the initial and remaining COD concentrations, respectively.

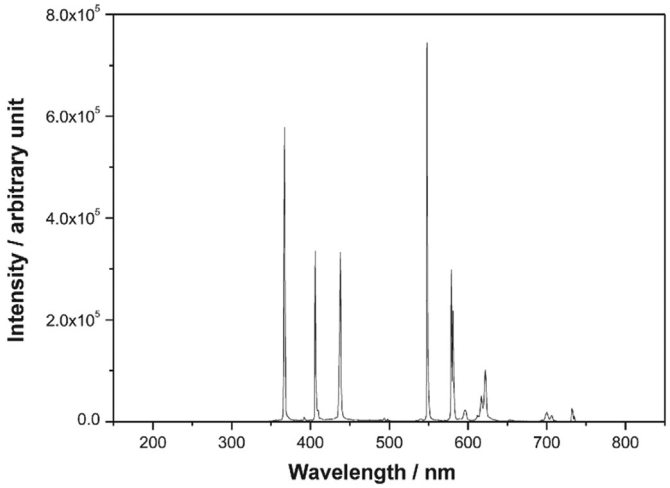

Figure 1. The emission spectrum of OSRAM HQL 125 W mercury vapor lamp used in the study. Reproduced with permission from [27]. Copyright Elsevier.

$$\%\ COD\ degradation = \frac{(COD_0 - COD)}{COD_0} \times 100 \quad (1)$$

3. Results and discussion

3.1. Statistical analysis and modeling

SWW was treated by TiO_2 photocatalysis under different conditions according to RSM. Statistical-based designs such as BBD are often used to understand complex systems such as wastewater degradation by allowing the simultaneous analysis of several factors and their interaction with a reasonable number of experiments [29]. Moreover, these methods also enable the generation of mathematical models that can be used to predict the response of the treatment process. Based on this, the second-order polynomial represented in Eq. (2). was fitted to the experimental values presented in Table 2 to infer the combined effects of the three factors studied. The model yields the efficiency of COD degradation (%) as a function of Photocatalyst dosage (X_1), Wastewater concentration (X_2), and Irradiation time (X_3).

$$\begin{aligned} Y_1(\text{COD removal }\%) = {} & 61.96 + 2.61\ X_1 - 15.33\ X_2 + 1.97\ X_3 \\ & - 2.80\ X_1X_2 + 1.33\ X_1X_3 - 0.075\ X_2X_3 - 0.542\ {X_1}^2 \\ & + 5.34\ {X_2}^2 - 6.93\ {X_3}^2 \end{aligned} \quad (2)$$

The equation indicates that the main effects of factor X_2 (Wastewater concentration) and the quadratic effects of X_2 and X_3 (Irradiation Time) were the most significant for COD reduction ($p < 0.05$). Factor X_1 may be significant ($p = 0.054$) but is less critical, while the remaining factor interactions and quadratic effects of X_1 have no significant effect on the treatment process ($p > 0.05$). ANOVA was used to determine the fit of the modeling procedure (Table 3). According to the analysis, the polynomial model was eligible to represent the actual relationship between the response (COD reduction) and the variables, with small p-value (0.000842), high adjusted R-squared (0.9478) and insignificant lack of fit (0.21). Figure 3 presents a comparison between observed and predicted values for COD removal. The statistical indicators R^2, root mean square (RMSE) and mean absolute error (MAE) are also shown in the figure and suggest the good predictive capability of the model.

3.2. Effect of variables on COD removal

During the photochemical degradation of SWW, pollutant removal may proceed primarily due to organics oxidation at the TiO_2 surface utilizing hydroxyl radicals formed from the reaction between photogenerated holes and adsorbed water. The mechanism of generation of these strong oxidants is described in the following equations [8, 30, 31]:

Photon absorption with sufficient energy promotes an electron from the valence band (VB) to the conduction band (CB), thus leading to the formation of an electron/hole pair

$$TiO_2 + h\vartheta \rightarrow e^-_{CB} + h^+_{VB} \quad (3)$$

Oxidation of the water present in the medium by the hole produced in the VB, thus forming $^{\bullet}OH$

$$h^+_{VB} + H_2O \rightarrow TiO_2 + H^+ + {}^{\bullet}OH \quad (4)$$

Reduction of oxygen by the electron promoted to the CB, thus forming superoxide radicals

$$e^-_{CB} + O_2 \rightarrow TiO_2 + O_2^{\bullet -} \quad (5)$$

The formed $^{\bullet}OH$ attacks organics, thus degrading these compounds into carbon dioxide and water

$$organics + {}^{\bullet}OH \rightarrow Intermediate\ products \rightarrow CO_2 + H_2O \quad (6)$$

In practice, organic pollutants are required to mass transfer from the bulk solution into the TiO_2 surface where they are adsorbed and

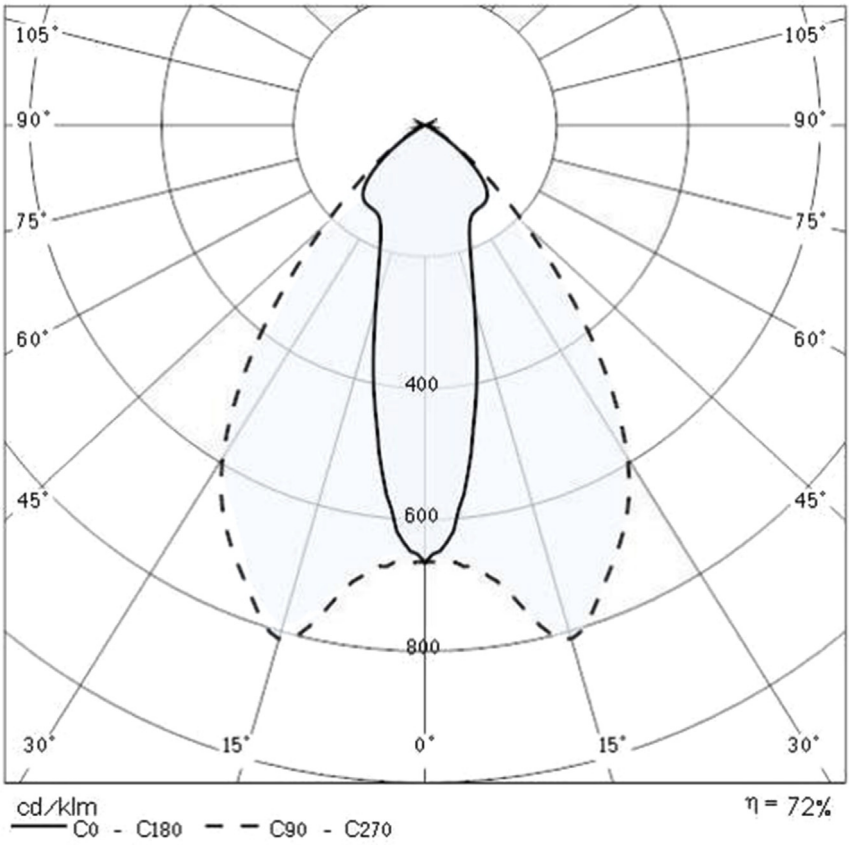

Figure 2. The light distribution curve of the SBP Jolly 2/S light fixture.

Table 2. Design matrix, observed response, and predicted values for the removal of COD from swine wastewater using heterogeneous photocatalysis.

Run	Independent Variables			Response (Y, %)		
	X_1 (g L^{-1}) Photocatalyst dosage	X_2 (%) Wastewater concentration	X_3 (h) Irradiation Time	Experimental	Predicted	Difference
				COD removal (%)		
1	1.5	3.125	9	85.6	88.5	(2.90)
2	1	9.375	6	41.5	43.2	(1.70)
3	0.5	3.125	9	76.9	77.7	(0.80)
4	1	9.375	12	45.0	47.0	(2.00)
5	1	6.25	9	61.4	62.0	(0.60)
6	1	6.25	9	64.0	62.0	2.00
7	0.5	6.25	6	51.1	52.3	(1.20)
8	1	6.25	9	60.5	62.0	(1.50)
9	0.5	6.25	12	52.7	53.6	(0.90)
10	1	3.125	6	75.6	73.6	2.00
11	1.5	6.25	6	55.8	54.9	0.90
12	1.5	6.25	12	62.7	61.5	1.20
13	1.5	9.375	9	53.2	52.4	0.80
14	0.5	9.375	9	55.7	52.8	2.90
15	1	3.125	12	79.4	77.7	1.70

photocatalyzed into products. Desorption then occurs, and the formed intermediates transfer from the interface region to the bulk liquid [32].

A preliminary analysis of the results reveals that the highest and lowest COD removals were achieved by runs 1 and 2, respectively, where 85.6% and 41.5% of COD was removed under different factor levels. As a comparison, for example, photolytic degradation (no TiO_2 added) only yielded 4% COD reduction, thus proving that photocatalyst addition enables the removal of pollutants. The 3D response surfaces in Figures 4, 5, and 6 provide additional insights concerning the variation and interaction between the factors studied; their analysis is provided in the following sections.

3.2.1. *Effect of photocatalyst dosage*

Figures 4 and 5 are of interest to understand the effect of added photocatalyst dosage on the degradation of SWW as measured by COD. The efficiency of degradation increased with an increase in photocatalyst

Table 3. ANOVA for the quadratic model used for the analysis of COD decay using BBD design.

	df	Sum of squares	Mean square	F-value	p-value	Remarks
FO (X_1,X_2,X_3)	3	1949.36	649.79	74.5695	0.0001428	Significant
TWI (X_1,X_2,X_3)	3	38.41	12.80	1.4691	0.3291343	Non-significant
PQ (X_1,X_2,X_3)	3	307.30	102.43	11.7552	0.0105660	Significant
Residuals	5	43.57	8.71			
Lack of fit	3	36.96	12.32	3.728	0.2186005	Non-significant
Pure error	2	6.61	3.30			

Multiple *R*-squared: 0.9814, Adjusted *R*-squared: 0.9478. *F*-statistic: 29.26 on 9 and 5 DF, *p*-value: 0.000842. FO: first order; TWI: two-way interaction; PQ: pure quadratic.

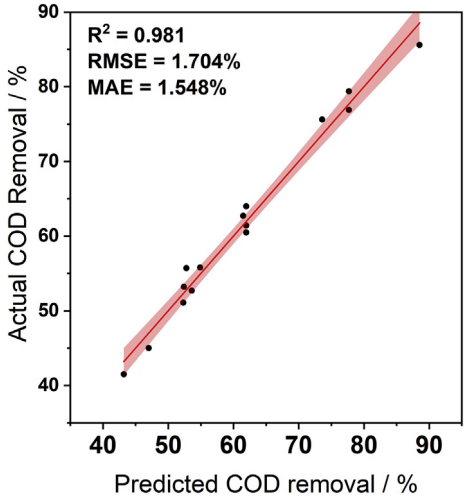

Figure 3. Actual versus predicted values for COD removal using Box-Behnken design.

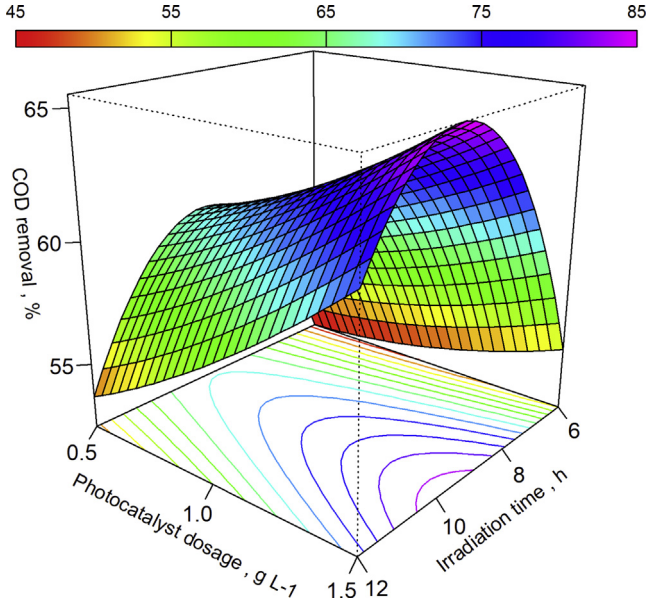

Figure 4. Response surface plot showing the interaction between X_1 (Photocatalyst dosage) and X_3 (Irradiation time) with the remaining factor fixed at the center level.

concentration. For all treatment conditions, the treatment with 1.5 g L^{-1} of TiO_2 under the artificial radiation of a 125W mercury lamp was more efficient than lower TiO_2 dosages (0.5 and 1.0 g L^{-1}). These results are probably due to the higher amount of hydroxyl radicals formed at higher photocatalyst dosages. In fact, as the number of active sites available increases due to more photo-generated electron-holes, the higher the oxidants produced, which results in increasing removal efficiency [31, 33]. On the other hand, issues with light penetration at higher catalyst dosages have been reported. These difficulties mean that higher levels of TiO_2 in suspension may hinder the treatment as the photo-activated volume of the semiconductor suspensions becomes smaller [9]. However, for the factor levels used in the present study, this effect was not observed, i.e., the optimal photocatalyst dosage was not exceeded.

3.2.2. Effect of wastewater concentration

Figures 5 and 6 show the interaction between wastewater concentration and the remaining factors. As can be seen in both figures, COD reduction is highly dependent on wastewater concentration, which means that the highest level for this factor led to a more efficient treatment. In particular, results suggest that wastewater concentrations above 3.125% may cause photocatalytic efficiency to decrease due to lower light transmission or penetration [6]. Moreover, these effects can also be rationalized in terms of the abundance of organic molecules in less diluted solutions (higher initial COD) as compared to the concentration of oxidant species formed during the photocatalytic process. This high concentration of organic compounds may lead to the deactivation of active sites in the photocatalyst due to the slow diffusion of intermediates (catalyst surface saturation) [34], as also suggested by the FTIR spectra of recovered photocatalyst particles (see also section 3.4).

3.2.3. Effect of irradiation time

Figures 4 and 6 represent the interaction between irradiation time and the other factors included in the experimental design. The progress of time under irradiation generally led to higher organics degradation; however, the photocatalytic process was less efficient after 9 h probably due to the slow reaction of more complex organic compounds with OH^- radicals and the short life-time of the photocatalyst because of active sites deactivation [9].

3.3. Optimal conditions and kinetics study

RSM can estimate the combination of factor levels which result in the highest percentage of COD degradation. Using the ridge analysis function in the RSM package of R software, the optimal conditions for COD reduction (98.1 %) were found to be a photocatalyst dosage of 1.16 g L^{-1}, wastewater concentration of 1.68 % and an irradiation time of 9.2 h. Under these optimal conditions, 91.7 % COD removal was obtained in a validation experiment, which is in good agreement with the response predicted by the model.

A kinetic analysis was also developed by monitoring COD decay as a function of irradiation time. Photodegradation of swine wastewater was found to fit well with the Langmuir-Hinshelwood (L-H) model and also confirms previous findings that the photocatalytic degradation of organic pollutants generally follows the L-H kinetics [11, 20, 23, 35, 36]. Assuming a first-order reaction, the L-H model can be simplified into the following equation:

$$\ln\frac{C_0}{C_T} = k_{app}t \tag{7}$$

where C_0 and C_T (mg.L^{-1}) are the initial and remaining COD in SWW, respectively, t (min) is the irradiation time, and k_{app} (min^{-1}) is the pseudo-first-order constant which corresponds to the degradation rate of the studied photocatalytic system.

Figure 7 shows the COD removal from SWW as a function of time at optimized conditions. The inset of Figure 7 confirms the first-order

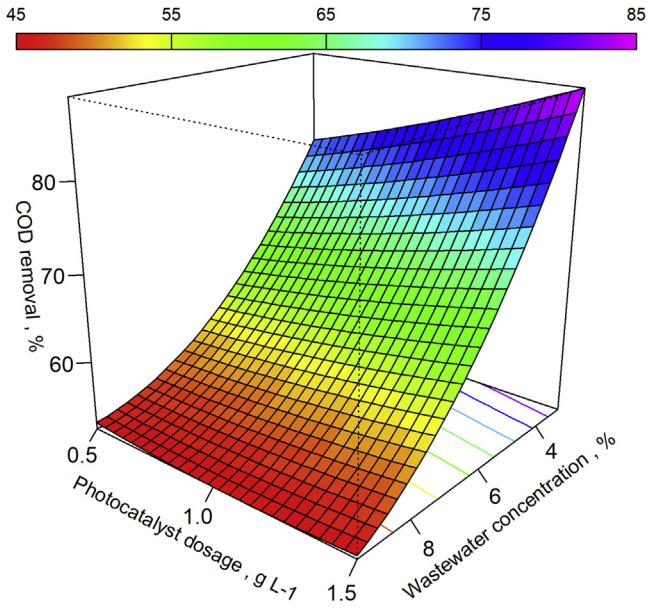

Figure 5. Response surface plot showing the interaction between X_1 (Photocatalyst dosage) and X_2 (Wastewater concentration) with the remaining factor fixed at the center level.

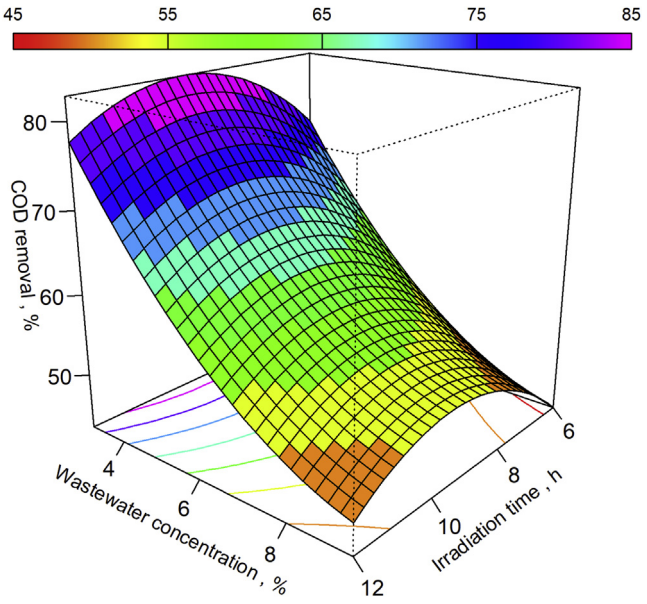

Figure 6. Response surface plot showing the interaction between X_2 (Wastewater concentration) and X_3 (Irradiation time) with the remaining factor fixed at the center level.

kinetics of the photodegradation reaction and allows to determine the pseudo-first-order kinetic constant (k_{app}) for the experiment. The photocatalytic reaction rate was found to be 3.9×10^{-3} min^{-1}, which is in good agreement with the findings of Subramonian et al. [23]. These authors studied the kinetics of photodegradation of pulp and paper mill wastewater by using several photocatalysts, including Aeroxide® TiO_2 P25.

3.4. TiO_2 reusability

Photocatalyst samples recovered from experiments were analyzed by FTIR and compared with pure Aeroxide® TiO_2 P25 to provide some insights on the reusability of the catalyst after treatment. The spectra presented in Figure 8 infers some structural changes in the catalysts, which may be attributed to the photocatalytic process. As inset, the spectra of untreated SWW is also shown for comparison. Peaks at 3300 cm^{-1} and 2927 cm^{-1} could be attributed to $-NH_2$ or –OH compounds and to the stretching vibration of C–H bond, respectively, and probably relate either to OH bending vibrations of absorbed water molecules or peptides, polyalcohols, and carbohydrates present in the wastewater [37]. Other peaks signals can also be identified in the regions near 1645 cm^{-1} and 1540 cm^{-1}, which may reflect asymmetrical vibrations of COO^- and symmetrical vibrations of NH^+ bonds. Both are characteristic of peptides and proteins which are usually present in wastewaters from animal origin but may also be ascribed to surface hydroxyls on the TiO_2 particles [37, 38]. Bands near 1056 cm^{-1} may, in turn, be attributed to the C–O–C stretching of polysaccharides [37, 39]. Finally, the broad peak in the range of 750–600 cm^{-1} has been attributed to the stretching vibration of Ti–O and is observed in all catalyst samples while being absent in the raw wastewater [38]. Peak signals are slightly reduced for the photocatalysts recovered from solutions with low wastewater concentration (3.125 %, and 6.45%), thus suggesting that catalyst reusability is possible; however, that may not be the case for the SWW solution with the higher initial COD (9.375%).

4. Conclusions

In this study, the treatability of SWW by photocatalytic degradation was tested over suspended Aeroxide® TiO_2 particles irradiated by artificial light and proved successful. RSM and BBD statistical techniques were adequately applied for the optimization of the operational parameters relevant to the process. The effects of photocatalyst dosage (X_1), wastewater concentration (X_2), and irradiation time (X_3) were studied by fitting a second-order polynomial and found to influence COD removal. The single effects of X_2 were negative and the most significant, while the effects of X_1 and X_3 were positive but considered less relevant. The quadratic effects of X_2 and X_3 were also crucial for COD reduction. ANOVA showed that the proposed model is acceptable with an adjusted $R^2 = 0.9666$. Based on the modeling, the optimal conditions for COD removal were a photocatalyst dosage of 1.16 g L^{-1}, a wastewater

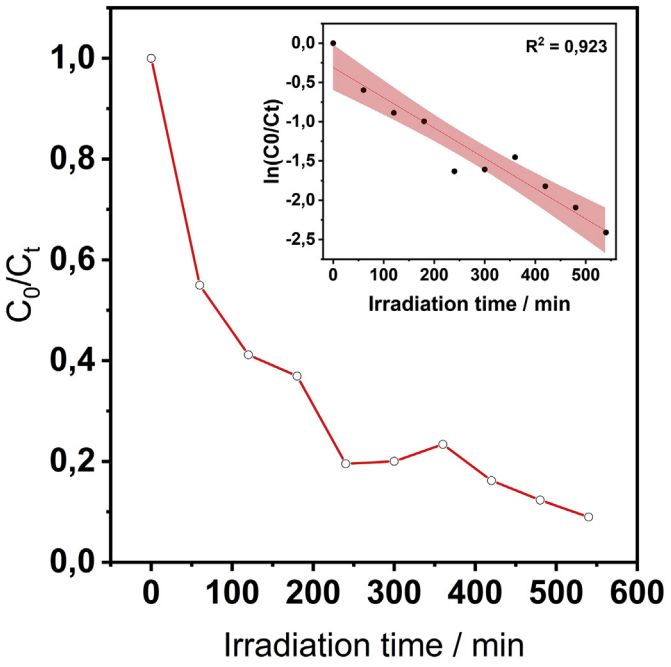

Figure 7. COD removal as a function of time in optimal conditions. Inset: Langmuir-Hinshelwood model of the photocatalytic degradation of SWW.

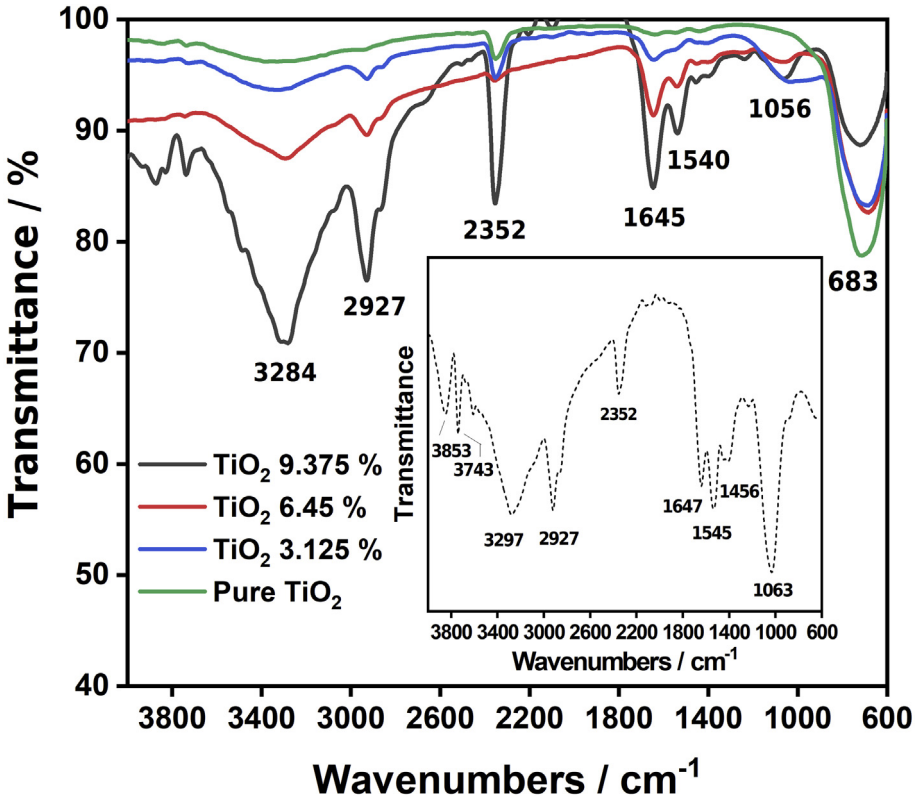

Figure 8. FTIR spectra of recovered Aeroxide® TiO_2 samples. Inset: FTIR spectrum of raw swine wastewater.

concentration of 1.68% and an irradiation time of 9.2 h. These conditions enabled a 91.7 % COD removal in a confirmation experiment. The kinetic analysis of the photodecomposition of SWW showed that COD decay fitted well the pseudo-first-order according to Langmuir—Hinshelwood model (reaction rate constant of 3.9×10^{-3} min^{-1}). Furthermore, FTIR analysis indicated that Aeroxide® TiO_2 was chemically stable after experiments and that catalyst reuse is possible for low wastewater concentrations. The results demonstrate that heterogeneous photocatalysis by using commercial TiO_2 as the photocatalyst may be a possible technology for the integrated treatment of industrial effluents that result from swine production, especially as post-treatment or as a polishing step due to the need for wastewater dilution. Future work to clarify the main active species and degradation products involved in the photooxidation of SWW, as well as more experiments with novel photocatalysts, would help photocatalytic technology to be implemented in practice.

Declarations

Author contribution statement

Bruno B. Garcia: Performed the experiments; Analyzed and interpreted the data; Wrote the paper.

Gonçalo Lourinho: Conceived and designed the experiments; Analyzed and interpreted the data; Wrote the paper.

Pedro Romano, Paulo S. D. Brito: Conceived and designed the experiments; Analyzed and interpreted the data.

Funding statement

This work was supported by the projects 0008_ECO2CIR_4_E and 0049_INNOACE_4_E co-funded by Interreg V-A Spain-Portugal Cooperation Programme (POCTEP). G. Lourinho was supported by FCT-Fundação para a Ciência e Tecnologia (grant SFRH/BDE/111878/2015).

Competing interest statement

The authors declare no conflict of interest.

Additional information

No additional information is available for this paper.

References

[1] S. Lopez-Ridaura, H. van der Werf, J.M. Paillat, B. Le Bris, Environmental evaluation of transfer and treatment of excess pig slurry by life cycle assessment, J. Environ. Manag. 90 (2009) 1296–1304.

[2] J.W. De Vries, A.J.A. Aarnink, P.W.G. Groot Koerkamp, I.J.M. De Boer, Life cycle assessment of segregating fattening pig urine and feces compared to conventional liquid manure management, Environ. Sci. Technol. 47 (2013) 1589–1597.

[3] D. Nierenberg, Global Meat Production and Consumption Continue to Rise, Worldwatch Inst., 2011.

[4] C.A. Villamar, T. Cañuta, M. Belmonte, G. Vidal, Characterization of swine wastewater by toxicity identification evaluation methodology (TIE), water, air, Soil Pollut. 223 (2012) 363–369.

[5] M.S. Lucas, R. Mosteo, M.I. Maldonado, S. Malato, J.A. Peres, Solar photochemical treatment of winery wastewater in a CPC reactor, J. Agric. Food Chem. 57 (2009) 11242–11248.

[6] Y. Lin, M. Mehrvar, Photocatalytic treatment of an actual confectionery wastewater using Ag/TiO2/Fe2O3: optimization of photocatalytic reactions using surface response methodology, Catalysts 8 (2018) 409.

[7] N. Chaibakhsh, N. Ahmadi, M.A. Zanjanchi, Optimization of photocatalytic degradation of neutral red dye using TiO 2 nanocatalyst via Box-Behnken design, Desalination Water Treat. 57 (2016) 9296–9306.

[8] C.G. Maia, A.S. Oliveira, E.M. Saggioro, J.C. Moreira, Optimization of the photocatalytic degradation of commercial azo dyes in aqueous TiO2 suspensions, React. Kinet. Mech. Catal. 113 (2014) 305–320.

[9] M.H. Habibi, A. Hassanzadeh, S. Mahdavi, The effect of operational parameters on the photocatalytic degradation of three textile azo dyes in aqueous TiO2 suspensions, J. Photochem. Photobiol. Chem. 172 (2005) 89–96.

[10] M. Jiménez, M. Ignacio Maldonado, E.M. Rodríguez, A. Hernández-Ramírez, E. Saggioro, I. Carra, J.A. Sánchez Pérez, Supported TiO2 solar photocatalysis at semi-pilot scale: degradation of pesticides found in citrus processing industry wastewater, reactivity and influence of photogenerated species, J. Chem. Technol. Biotechnol. 90 (2015) 149–157.

[11] K. Sirirerkratana, P. Kemacheevakul, S. Chuangchote, Color removal from wastewater by photocatalytic process using titanium dioxide-coated glass, ceramic tile, and stainless steel sheets, J. Clean. Prod. 215 (2019) 123–130.
[12] N. Malesic-Eleftheriadou, E. Evgenidou, G.Z. Kyzas, D.N. Bikiaris, D.A. Lambropoulou, Removal of antibiotics in aqueous media by using new synthesized bio-based poly(ethylene terephthalate)-TiO2 photocatalysts, Chemosphere 234 (2019) 746–755.
[13] A. Cabrera-Reina, A.B. Martínez-Piernas, Y. Bertakis, N.P. Xekoukoulotakis, A. Agüera, J.A. Sánchez Pérez, TiO2 photocatalysis under natural solar radiation for the degradation of the carbapenem antibiotics imipenem and meropenem in aqueous solutions at pilot plant scale, Water Res. 166 (2019) 115037.
[14] J. Ge, Y. Zhang, Y.-J. Heo, S.-J. Park, Advanced design and synthesis of composite photocatalysts for the remediation of wastewater: a review, Catalysts 9 (2019) 122.
[15] X. Li, J. Xiong, X. Gao, J. Ma, Z. Chen, B. Kang, J. Liu, H. Li, Z. Feng, J. Huang, Novel BP/BiOBr S-scheme nano-heterojunction for enhanced visible-light photocatalytic tetracycline removal and oxygen evolution activity, J. Hazard Mater. (2019) 121690.
[16] J. Wang, Q. Zhang, F. Deng, X. Luo, D.D. Dionysiou, Rapid toxicity elimination of organic pollutants by the photocatalysis of environment-friendly and magnetically recoverable step-scheme SnFe2O4/ZnFe2O4 nano-heterojunctions, Chem. Eng. J. 379 (2020) 122264.
[17] F. Deng, X. Lu, Y. Luo, J. Wang, W. Che, R. Yang, X. Luo, S. Luo, D.D. Dionysiou, Novel visible-light-driven direct Z-scheme CdS/CuInS2 nanoplates for excellent photocatalytic degradation performance and highly-efficient Cr(VI) reduction, Chem. Eng. J. 361 (2019) 1451–1461.
[18] H. Li, F. Deng, Y. Zheng, H. Li, C. Qu, X. Luo, Visible-light-driven Z-scheme rGO/Bi2S3-BiOBr heterojunction with tunable exposed BiOBr (102) facets for efficient synchronous photocatalytic degradation of 2-nitrophenol and Cr(VI) reduction, Environ. Sci. Nano. (2019) 3670–3683.
[19] E.M. Saggioro, A.S. Oliveira, D.F. Buss, D.D.P. Magalhães, T. Pavesi, M. Jimenéz, M.I. Maldonado, L.F.V. Ferreira, J.C. Moreira, Photo-decolorization and ecotoxicological effects of solar compound parabolic collector pilot plant and artificial light photocatalysis of indigo carmine dye, Dyes Pigments 113 (2015) 571–580.
[20] A. Mirzaei, L. Yerushalmi, Z. Chen, F. Haghighat, J. Guo, Enhanced photocatalytic degradation of sulfamethoxazole by zinc oxide photocatalyst in the presence of fluoride ions: optimization of parameters and toxicological evaluation, Water Res. 132 (2018) 241–251.
[21] A. Mirzaei, L. Yerushalmi, Z. Chen, F. Haghighat, Photocatalytic degradation of sulfamethoxazole by hierarchical magnetic ZnO@g-C3N4: RSM optimization, kinetic study, reaction pathway and toxicity evaluation, J. Hazard Mater. 359 (2018) 516–526.
[22] H. Ates, N. Dizge, H.C. Yatmaz, Combined process of electrocoagulation and photocatalytic degradation for the treatment of olive washing wastewater, Water Sci. Technol. 75 (2017) 141–154.
[23] W. Subramonian, T.Y. Wu, S.-P. Chai, Photocatalytic degradation of industrial pulp and paper mill effluent using synthesized magnetic Fe 2 O 3 -TiO 2 : treatment efficiency and characterizations of reused photocatalyst, J. Environ. Manag. 187 (2017) 298–310.
[24] D.M. Tobaldi, R.C. Pullar, M.P. Seabra, J.A. Labrincha, Fully quantitative X-ray characterisation of Evonik Aeroxide TiO 2 P25®, Mater. Lett. 122 (2014) 345–347.
[25] K.W. John Fox, Milan Bouchet-Valat, Liviu Andronic, Michael Ash, Theophilius Boye, Stefano Calza, Andy Chang, Philippe Grosjean, Richard Heiberger, Kosar Karimi Pour, G.Jay Kerns, L. Renaud, Rcmdr: R commander, R package version 2.6-0, 2010.
[26] S. Bhavsar, P. Dudhagara, S. Tank, R software package based statistical optimization of process components to simultaneously enhance the bacterial growth, laccase production and textile dye decolorization with cytotoxicity study, PloS One 13 (2018) 1–18.
[27] M. Richena, C.A. Rezende, Effect of photodamage on the outermost cuticle layer of human hair, J. Photochem. Photobiol. B Biol. (2015).
[28] APHA/AWWA/WEF, Standard methods for the examination of water and wastewater, Stand. Methods (2012) 541.
[29] B. yul Tak, B. sik Tak, Y. ju Kim, Y. jin Park, Y. hun Yoon, G. ho Min, Optimization of color and COD removal from livestock wastewater by electrocoagulation process: application of Box-Behnken design (BBD), J. Ind. Eng. Chem. 28 (2015) 307–315.
[30] E.V. dos Santos, O. Scialdone, Photo-electrochemical technologies for removing organic compounds in wastewater, in: Electrochem. Water Wastewater Treat., Elsevier, 2018, pp. 239–266.
[31] E.M. Saggioro, A.S. Oliveira, J.C. Moreira, Heterogeneous photocatalysis remediation of wastewater polluted by indigoid dyes, in: Text. Wastewater Treat., InTech, 2016.
[32] M.N. Chong, B. Jin, C.W.K. Chow, C. Saint, Recent developments in photocatalytic water treatment technology: a review, Water Res. 44 (2010) 2997–3027.
[33] X. Lin, A. Yang, G. Huang, X. Zhou, Y. Zhai, X. Chen, E. McBean, Treatment of aquaculture wastewater through chitin/ZnO composite photocatalyst, Water 11 (2019) 310.
[34] J.C. Costa, M.M. Alves, Posttreatment of olive mill wastewater by immobilized TiO 2 photocatalysis, Photochem. Photobiol. 89 (2013) 545–551.
[35] M. Długosz, P. Zmudzki, A. Kwiecień, K. Szczubiałka, J. Krzek, M. Nowakowska, Photocatalytic degradation of sulfamethoxazole in aqueous solution using a floating TiO2 expanded perlite photocatalyst, J. Hazard Mater. 298 (2015) 146–153.
[36] Z. Khuzwayo, E.M.N. Chirwa, Modelling and simulation of photocatalytic oxidation mechanism of chlorohalogenated substituted phenols in batch systems: Langmuir-Hinshelwood approach, J. Hazard Mater. 300 (2015) 459–466.
[37] M. Kowalski, K. Kowalska, J. Wiszniowski, J. Turek-Szytow, Qualitative analysis of activated sludge using FT-IR technique, Chem. Pap. 72 (2018) 2699–2706.
[38] A.T. Kuvarega, R.W.M. Krause, B.B. Mamba, Comparison between base metals and platinum group metals in nitrogen, M codoped TiO2 (M = Fe, Cu, Pd, Os) for photocatalytic removal of an organic dye in water, J. Nanomater. 2014 (2014).
[39] M.J. Cuetos, A. Morán, M. Otero, X. Gómez, Anaerobic co-digestion of poultry blood with OFMSW: FTIR and TG-DTG study of process stabilization, Environ. Technol. 30 (2009) 571–582.